COMPUTATIONAL ANALYSIS OF LOCALLY FORCED FLOW OVER A WALL-MOUNTED HUMP AT HIGH-RE NUMBER

S. Šarić, S. Jakirlić and C. Tropea
Chair of Fluid Mechanics and Aerodynamics,
Darmstadt University of Technology
Petersenstr. 30, D-64287 Darmstadt, Germany
saric@sla.tu-darmstadt.de, s.jakirlic@sla.tu-darmstadt.de, ctropea@sla.tu-darmstadt.de

ABSTRACT

An incompressible, high-Reynolds number flow (slightly less then 1 Mio. per chord) over a smoothly contoured wall-mounted hump was studied computationally by using the LES (Large Eddy Simulation) and DES (Detached Eddy Simulation) methods. In addition the Spalart-Allmaras model within the RANS (Reynolds-Averaged Navier-Stokes) framework was tested. The focus of the investigation was on the effects of the local perturbation of the hump boundary layer introduced by the spatially uniform (in the spanwise direction) steady suction and oscillatory suction/blowing through a narrow opening ($4mm$) situated at the hump crest immediately upstream of the natural separation point. Reference experiments have shown that both flow control mechanisms cause a shortening of the recirculation bubble relative to the baseline configuration (no flow control). The LES method, despite the coarse mesh (with a total of 4 Mio. cells) for this high Reynolds number, wall-bounded flow, was capable of capturing important effects of the flow control qualitatively and quantitatively, whereas DES failed to do so, inspite of superior results in the baseline case. A sensitivity study of the RANS-LES interface position within the DES approach shows that a RANS region chosen too thin (with the interface situated at the very beginning of the logarithmic layer) can lead to a strong reduction of the turbulent viscosity causing a low turbulence level within the shear layer region aligned with the recirculation zone, which in turn leads to a larger separation bubble.

INTRODUCTION

An important task in the fluid mechanics research is to control turbulent flow evolution with respect to overall drag reduction. Flow separation, often being the consequence of an adverse pressure gradient, is certainly one of the main flow phenomena contributing to increased drag. Therefore, separation delay or separation zone reduction is of great interest in a number of industrial branches, e.g. turbomachinery, car and aircraft aerodynamics, etc. There are different ways of active flow separation control; the most common are steady flow suction and periodic flow perturbation at the natural separation point. As examples, the following experimental investigations are noted: flows with a fixed separation point - flow over a backward-facing step (Chung and Sung, 1996; Jin et al., 2001; Yoshioka et al., 2001) - and separation from smooth surfaces - flow past an airfoil and over a hump (Seifert and Pack, 1999 and 2002). These flow configurations have recently attracted the attention of the CFD community. The periodically perturbed backward-facing step flow (Yoshioka et al.) served as a test case at the 9th ERCOFTAC workshop on refined turbulence modelling (Darmstadt University of Technology, 2001) and was recently computationally investigated by Šarić et al. (2004) and Dejoan et al. (2004). The turbulent flow over a wall-mounted hump (Fig. 1, simulating the upper surface of a Glauert-Goldschmied type airfoil at zero angle of attack) at high chord-based Reynolds number $Re_c = 936000$ (with free stream velocity $U_\infty = 34.6m/s$ and chord length $C = 0.42m$) situated in a plane channel (height $0.909C$) was experimentally re-examined at the NASA Langley Research Center (Greenblat et al., 2004, 2005) for the purpose of the CFDVAL workshop on computational methods and turbulence model validation (Gatski and Rumsey, 2004).

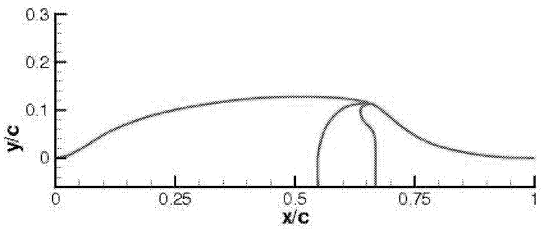

Figure 1: Schematic of the hump geometry

Hereby, three flow types were investigated: steady flow with no control (baseline) and two cases with flow control accomplished by steady suction through a thin slot situated at approximately 65% of the chord length, immediately upstream of the natural separation point, as well as by an alternating suction/blowing (zero net-mass-flow rate) of a jet into a boundary layer. The oncoming flow is characterized by a zero-pressure-gradient turbulent boundary layer, whose thickness δ is approximately 57% of the maximum hump height ($h_{\max} = 53.74$) measured at the location about two chord lengths upstream of the hump leading edge, corresponding to the momentum-thickness-based Reynolds number $Re_\theta \approx 7700$. The latter result was obtained by applying a near-wall, second-moment closure model, Fig. 2.

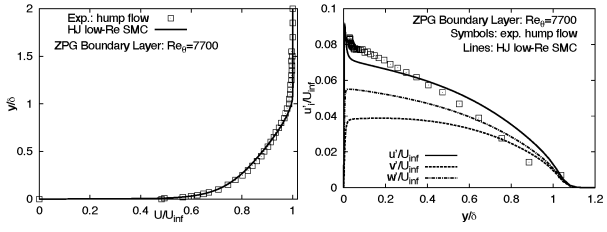

Figure 2: Mean velocity and Reynolds stresses at $x/c = -2.14$

The latter flow configurations were considered also in the present work. The purpose was the computational study of the effects of the boundary layer forcing on the mean flow and turbulence using various methods for unsteady flow computations: LES (Large Eddy Simulation), DES (Detached Eddy Simulations) and RANS (Reynolds-Averaged Navier-Stokes) aiming also at mutual comparison of their features and performance in such a complex flow situation.

COMPUTATIONAL METHOD

All computations were performed with an in-house computer code FASTEST 3D (Flow Analysis by Solving Transport Equations Simulating Turbulence) based on a finite volume numerical method for solving both three-dimensional filtered and Reynolds-Averaged Navier-Stokes equations on block-structured, body-fitted, non-orthogonal meshes. The computer code is parallelized applying the Message Passing Interface (MPI) technique for communication between the processors. The sub-grid scales were modeled by the most widely used model formulation proposed by Smagorinsky (1963) for the LES computations. A one-equation turbulence model by Spalart and Allmaras (S-A, 1994), based on the transport equation for turbulent viscosity, was employed to model the influence of the smallest, unresolved scales on the resolved ones for the DES computational scheme (e.g. Travin et al., 2002). The above-mentioned S-A turbulence model was also appled in the RANS mode. It was interesting to see how the same model performed in two different computational frameworks: RANS and DES. The convective transport of all variables was discretized by a second-order, central differencing scheme. Time discretization was accomplished by applying the (implicit) Crank-Nicolson scheme. The solution domain (dimensions: $6.14c$x$0.909c$x$0.152c$) is meshed with almost 4 Mio. (426x145x64) grid cells when applying the LES. A grid used in the 2D RANS calculations (426x145) was extruded in the spanwise direction to create 3D grid configurations used for LES and DES computations. The solution domain employed for DES with a somewhat larger spanwise dimension ($0.2c$), was meshed by approximately 1.7 Mio. (426x145x28) grid cells. The various RANS computations (not presented here) have not shown significant difference in the solutions obtained if the computation domain was extended further upstream ($6.39c$) as in the experiment. Therefore, in all the LES and DES computations available experimental velocity profiles were imposed at the inlet plane placed at $2.14c$ upstream of the hump leading edge, Fig. 2. This is in accordance with the results of the CFDVAL workshop on computational methods and turbulence model validation (Gatski and Rumsey, 2004). Furthermore, an important outcome of the workshop was that the modelling of the flow within the cavity/nozzle (Fig. 1) was not found to be critical for the flow predictions, as far as the baseline and steady suction flow control cases are concerned. S-A RANS computation of the baseline case, though not shown here, has shown that modelling of the cavity opening did not result in significant differences compared to the results presented here. Consequently, different flow configurations have been computed by imposing the appropriate boundary conditions directly at the control slot. Steady suction is achieved by adopting the spatially uniform suction velocity at the slot corresponding to the mass flow rate of $0.01518kg/s$. Oscillatory suction/blowing was simulated by imposing a sinusoidal zero net-mass-flow jet at the slot with the frequency of $138.5Hz$ and velocity amplitude of $26.6m/s$. The dimensionless time step of 0.005 (based on the hump chord length and free stream velocity) was used in the computations providing the CFL number less than unity throughout the largest portion of the solution domain. The only exception is the narrow region around the thin slot at the hump ($4mm$ width). Additionally, some preliminary simulations of the oscillatory blowing/suction case employing finer time steps (0.0016 and 0.003) reveal that the results were not significantly affected by the time step refinement. No-slip boundary conditions were applied at the walls ($y^+ < 1$), convective outflow at the outlet and periodic boundary conditions along the spanwise direction. The flow region of interest just downstream of the slot including the region arround the reattachment was meshed to provide $\Delta x^+ = 80$, $\Delta y^+ = 1 - 80$, $\Delta z^+ = 150$. The latter value applies to the DES grid. Compared to DES, the LES resolution was finer with $\Delta z^+ = 50$ because of a smaller spanwise domain size. Admittedly, the grid resolution adopted is coarser than it would be required for resolving the near-wall streaky structures, which demands a spacing of order $\Delta y^+ = O(1)$, $\Delta x^+ = O(50)$ and $\Delta z^+ = O(20)$, e.g. Hanjalic (2004). However, the employed resolution still provides modelled turbulent kinetic energy which does not exceed 5% to 9 % of the resolved one and the ratio of turbulent SGS viscosity to the molecular one remains typically between 5 to 13 (maximum values apply within the region arround the hump). The DES grid was designed based on experience with computations of some other flows; the main issue was to provide a proper position of the RANS-LES interface, i.e. to avoid that the interface penetrates too deeply into the boundary layer. If the LES region resides too close to the wall due to insufficient resolution (one would have actually a resolution typical for RANS in the LES region), lower viscosity and turbulence levels could be obtained, possibly causing a premature separation and poor flow predictions.

RESULTS AND DISCUSSION

The predictions of the separated flow over a wall-mounted hump for the configurations without flow control (baseline) and steady suction flow control will be discussed first. Afterwards some results for the case with sinusoidal suction/blowing flow control (oscillatory) will be presented as well. Flow statistics were taken over 5 to 7 flow-through times and the time-averaged results were extracted to provide comparison with the available experimental data. Predictions of the separation and reattachment locations for the computed configurations are summarized in Table 1 and Fig. 3.

Baseline configuration

Predictions of the pressure coefficient for the case without flow control are shown in Fig. 4. The LES and DES results agree better with the measurements than the 2D S-A RANS ones. However, the peak suction pressure is underpredicted with all methods. This can be partially explained by possible blockage effects through the wind tunnel side walls, not accounted for in the computations. The mean streamwise velocity profiles are shown in Figs. 5. The S-A RANS model overpredicts significantly the reattachment length inspite of correct capturing of the separation location (see Table 1 for the quantitative comparison). The LES and DES results agree well with the experimental data. It is interesting to see that

Table 1: Separation and reattachment locations

		$(x/C)_S$	$(x/C)_R$
Baseline	Exp.	0.673	1.110
	LES	0.667	1.114
	DES	0.663	1.121
	RANS S-A	0.667	1.259
Suction	Exp.	0.686	0.940
	LES	0.671	0.947
	DES	0.674	1.105
	RANS S-A	0.674	1.098
Oscillatory	Exp.	≈ 0.677	≈ 1.0
	LES	0.671	1.020
	DES	0.672	1.110

a) Baseline configuration

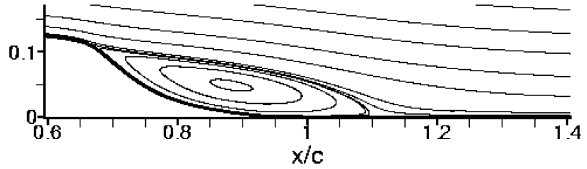

b) Steady suction configuration

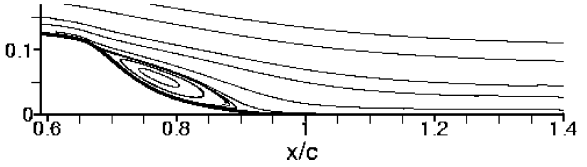

c) Oscillatory suction/blowing configuration

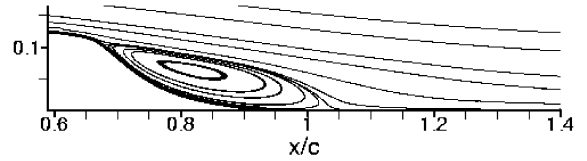

Figure 3: Time-averaged streamlines obtained by LES method

DES predictions are even better than the ones obtained by the conventional LES (see also the shear stress profiles in Fig. 7). The feasibility of the DES as a hybrid RANS/LES approach (designed to operate as the RANS method within attached boundary layers and the LES method in detached, separated regions of the flow) is further expressed through the fact, that these results were obtained using a substantially coarser grid (1.7 Mio. in total vs. 4 Mio. for LES). The Reynolds shear stress evolution presented in Fig. 6 demonstrates how crucial the proper level of turbulence in separated shear layer is with respect to the mean flow features downstream, especially to the reattachment location. A higher level of the shear stress implies an enhancement of the fluid entrainment into the shear layer - more intense momentum transport - and consequently a shorter recirculation bubble. The correct LES and DES predictions of the shear stress in the region aligned with the mean dividing streamline leads finally to the correct predictions of the reattachment length.

Steady Suction Flow Control

The pressure coefficient distributions for the steady suction flow control case are presented in Fig. 8. Underprediction of the peak suction pressure is present in the suction case as well.

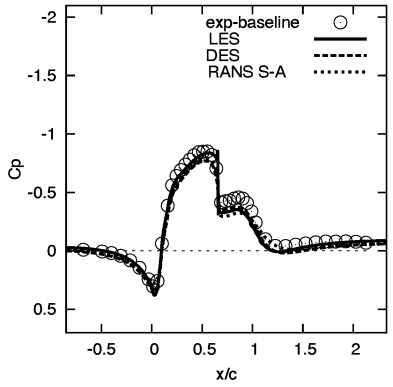

Figure 4: Pressure coefficient for the baseline configuration

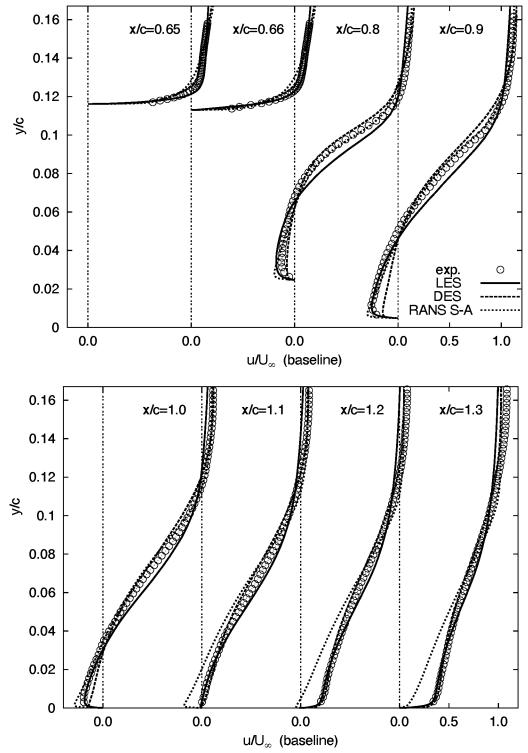

Figure 5: Mean velocity profiles (baseline configuration)

Contrary to the baseline case, the advantages of the DES over the S-A RANS predictions are not observed in the pressure distributions, noting that both S-A RANS and DES fail to capture the correct reattachment location, Table 1. On the other hand, LES shows very good agreement with the experimental data. The slight underpediction of the pressure coefficient along separation and recovery regions may be attributed to the afore mentioned blockage effects. Mean velocity profiles shown in Fig. 9 support previous observation made regarding the pressure distribution. The deviations from the experimental results with respect to the back-flow intensity within the recirculation bubble are clearly visible, influencing strongly the flow arround reattachment and in the recovery region downstream (it applies to S-A RANS and DES). LES predictions of the mean velocity are in a very good agreement with the experiment in spite of the slightly underpredicted separation location. Reynolds shear stress profiles are presented in Fig. 10. The intensification of the mean straining due to local

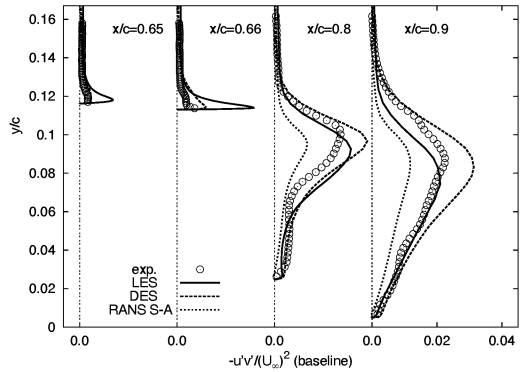

Figure 6: Shear stress profiles (baseline configuration)

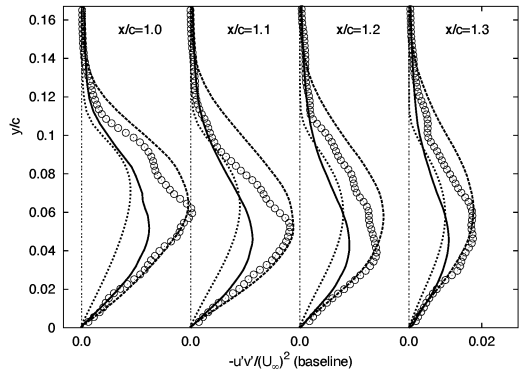

Figure 7: Shear stress profiles (baseline configuration)

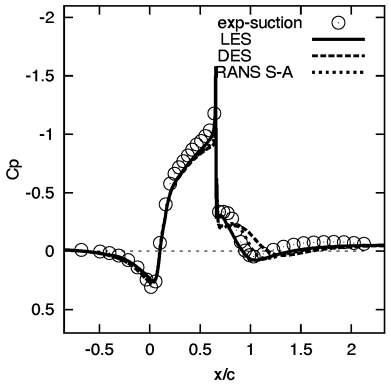

Figure 8: Pressure coefficient for the steady suction case

flow forcing in the suction case results in an enhanced turbulence level, representing the basic mechanisms behind the active flow control. Compared to S-A RANS and DES, LES captured the increased turbulence level in the separated shear layer region very well. Qualitatively different performance of the DES compared to the LES in two different flow configurations employing the same grid (DES performs very well in the baseline case, but very poor in the suction case) indicates the importance of the grid design within the DES framework. The issue of the RANS-LES interface, whose position is dictated by the grid adopted (independent of the flow structure), appears to be crucial for exploiting advantages of both RANS and LES strategies in different regions of the flow. The position of interface in terms of the wall units varies significantly in the separation region as shown in Fig. 11. The question arising is whether the grid used for the baseline case can be used for different flow scenarios, i.e. suction and oscillatory

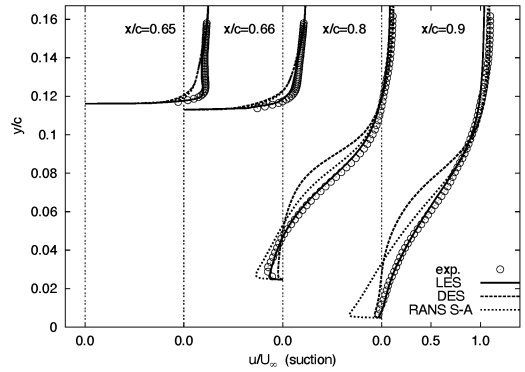

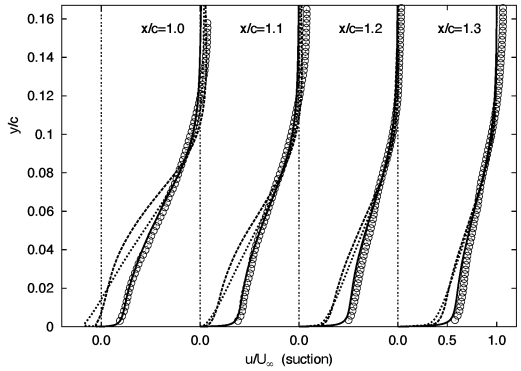

Figure 9: Mean velocity profiles (steady suction flow control) flow control?

Oscillatory Suction/Blowing Flow Control

In this section, some preliminary[1] results of the oscillatory case computations can be assessed. Fig. 14 displays the iso-surfaces of the vorticity (coloured by pressure) in the DES prediction of the oscillatory suction/blowing flow control (oscillatory case). The DES treatment of the separated region results in clearly visible resolved eddies downstream of the slot. The control mechanism of the oscillatory case turns out to be less effective than the one of steady suction, as observed in the experiment as far as the separation delay and recirculation zone shortening are concerned (Table 1). Reattachment length reduction is reproduced by LES, whereas DES ovepredicts the reattachment location, similar to the suction case. Fig. 12 displays the effects of the flow control on the mean velocity at two different stations, within the recirculation region ($x/c = 0.8$) and in the recovery region ($x/c = 1.1$). Experiments have shown that the shortening of the recirculation bubble by 42% and 26%, compared to the baseline case, is achieved by applying steady suction and oscillatory flow control respectively. LES predictions are in a fairly good agreement; the same tendency of the mean velocity field is achieved (Fig. 12), while shortening of the recirculation bubble is underpredicted: 38% and 22% for the two control mechanisms. Among the flow configurations considered, the oscillatory case appears to be the most challenging one. Different time steps were employed as mentioned before to perform LES and DES of the oscillatory case. Though results of the oscillatory case computations demonstrate generally good predictions of the recirculation bubble, i.e. both separation and

[1]The displayed, time-averaged results are obtained after 40 periods of the slot-flow oscillation. Further simulations are in progress.

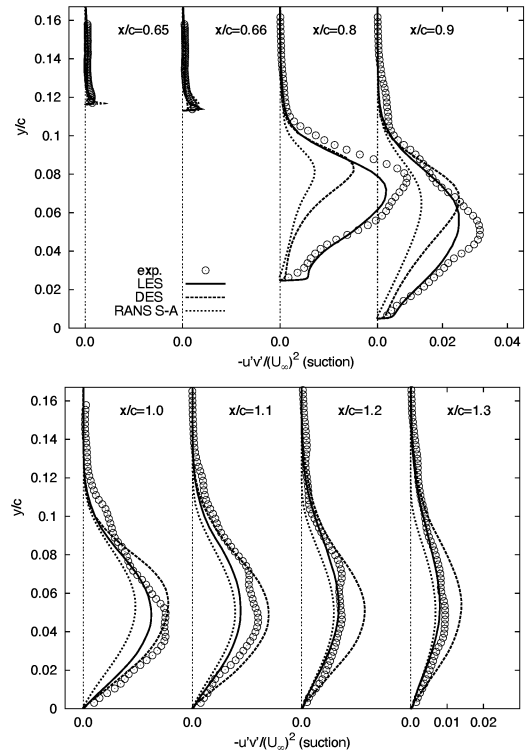

Figure 10: Shear stress profiles (steady suction flow control)

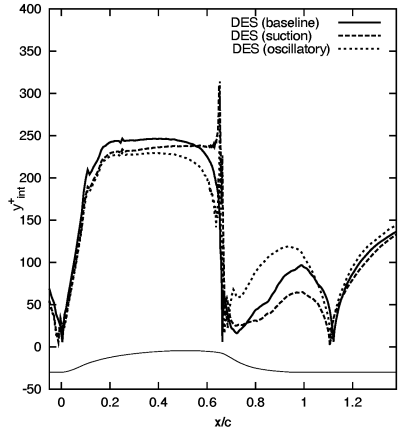

Figure 11: RANS-LES interface in DES computations

reattachment locations, the mean velocity profiles presented in Figs. 12 and 13 reveal less accurate predictions compared to the previous two cases. Different variants of Smagorinsky SGS model were tested: with and without van Driest damping of the Smagorinsky coefficient ($C_s = 0.1$) and the dynamic Smagorynski model of Germano et al. (1991). The results obtained by the dynamic procedure to determine C_s seem to be in better agreement with the experiment, the fact representing an expected outcome, knowing that a SGS model plays a more important role on an insufficiently fine grid. One of the experimentally observed features of the oscillatory case was that typically two to three vortices were present in the PIV-measurements region covering the entire separation bubble and the reattachment region up to $x/c = 1.3$ at any instant (Greenblatt et. al, 2005). This can be seen in Fig. 15, showing the instantaneous velocity field predictions by LES

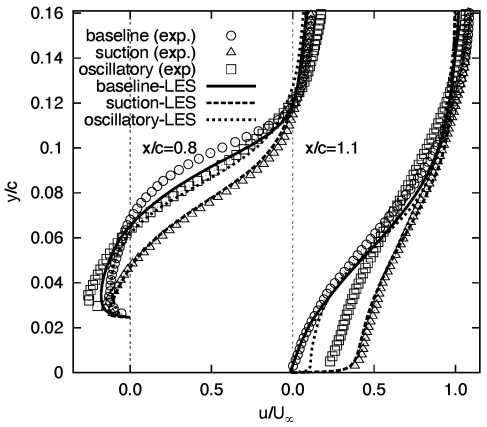

Figure 12: Effect of the flow control on the mean velocity profiles at x/c=0.8 and x/c=1.1 (LES vs experiment)

for different phase angles. It displays generation, rolling up and shedding of the vortices through the phase angles of 90° (blowing peak), 180° (switch from blowing to suction), 270° (suction peak) and 360° (switch from suction to blowing). By carefull inspection of the figure one can discern the movement of separation point as found in the experiment. At the instant corresponding to the blowing peak the local separation zone moves upstream towards the slot, the shear layer being lifted off the wall. As the suction peak is reached, the shear layer is pulled towards the wall and separation point moves downstream of the slot.

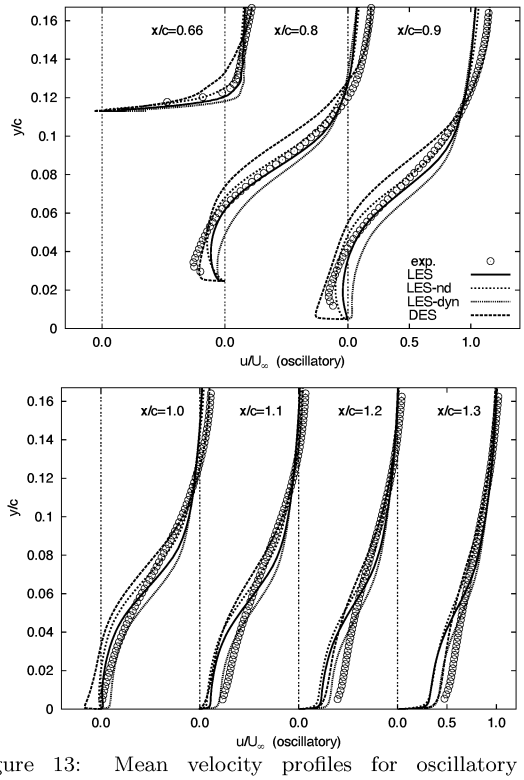

Figure 13: Mean velocity profiles for oscillatory suction/blowing flow control

CONCLUSIONS

Different computational approaches: LES (Large Eddy

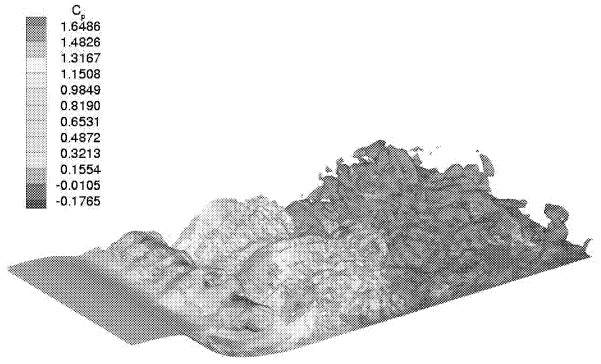

Figure 14: Vorticity iso-surfaces (coloured by pressure) obtained by DES of oscillatory suction/blowing flow control case)

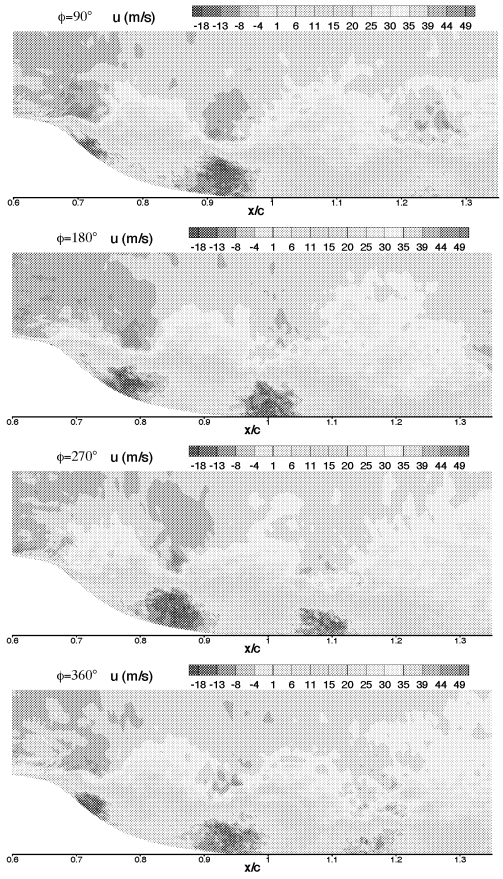

Figure 15: Instantaneous U-velocity field obtained by LES for various phase angles

Simulation), DES (Detached Eddy Simulations) and RANS (Reynolds-Averaged Navier-Stokes) were used to predict the flow over a wall-mounted hump aiming at mutual comparison of their features and performances in such a complex flow situations relevant to the active flow control. The LES and DES predictions of the main characteristics of separated flow over a wall-mounted hump, obtained on relatively coarse grids with respect to the flow Reynolds number considered ($Re_c = 9.36 \cdot 10^5$), are encouraging, outperforming significantly the S-A RANS. It is interesting to see that the DES results are almost identical to those obtained by using the conventional LES in the baseline case. It is especially encouraging when one knows that the substantially lower grid resolution (only 1.7 Mio. cells in total vs 4 Mio. cells for LES) was applied. However, poor performance in the suction case (LES superior to DES) indicates the importance of the DES grid design. The issue of RANS-LES interface appears to be crucial for exploiting advantages of both RANS and LES strategies in different regions of the flow. Comparison of the interface position in all three flow configurations gives a rise to a question whether a grid used for the baseline case can be used for different flow control scenarios, i.e. suction and oscillatory flow control? LES was capable to provide good predictions of the important effects of the steady suction and oscillatory suction/blowing flow control, that is the shortening of the recirculation bubble compared to the referent baseline case, wheras DES failed to do so inspite of satisfactory results in the baseline case. Some preliminary results of the oscillatory case computations demonstrate in general good predictions of the recirculation bubble, both instantaneously and in the time mean sense, but mean velocity field exhibits significant deviations from the experimental data. Among the flow configurations considered, the oscillatory case appears to be the most challenging one for the unsteady flow computational strategies like LES and DES.

Acknowledgements. The authors (S.Š.) gratefully acknowledge financial support of the Deutsche Forschungsgemeinschaft through the grants GK "Modelling and numerical description of technical flows" and the research group on "LES of complex flows" (FOR 507/1, JA 941/7-1).

REFERENCES

[1.] Chun, K.B., and Sung, H.J. (1996): Control of turbulent separated flow over a backward-facing step. *Experiments in Fluids*, Vol. 21, pp. 417-426

[2.] Dejoan, A., Jang, Y.-J., and Leschziner, M. (2004): LES and unsteady RANS computations for a periodically-perturbed separated flow over a backward-facing step. *ASME Heat Transfer/Fluids Engineering Summer Conference*, July 11-15, Charlotte, NC, USA

[3.] Gatski, T., and Rumsey, C. (2004): CFD Validation of Synthetic Jets and Turbulent Separation Control. Langley Research Center Workshop, Williamsburg, VA, USA, March 29-31

[4.] Hanjalić, K. (2004): Will RANS survive LES? *ASME Heat Transfer/Fluids Engineering Summer Conference*, July 11-15, Charlotte, NC, USA

[5.] Šarić, S., Jakirlić, S., and Tropea, C. (2004): A periodically-perturbed backward-facing step flow by means of LES, DES and T- RANS: an example of flow separation control. *ASME Heat Transfer/Fluids Engineering Summer Conference*, July 11-15, Charlotte, NC, USA

[6.] Seifert, A., and Pack, L.G. (2002): Active flow separation control on wall-mounted hump at high Reynolds numbers. *AIAA Journal*, Vol. 40, No. 7, pp. 1363-1372

[7.] Travin, A., Shur, M., Strelets, M., and Spalart, P.R. (2002): Physical and numerical upgrades in the Detached-Eddy Simulation of complex turbulent flow. In *Fluid Mechanics and its Application*, R. Friedrich and W. Rodi (Eds.), Vol. 65, pp. 239-254

[8.] Greenblatt, D., Paschal, K.B., Yao, C.S., and Harris, J., (2005): A separation control CFD validation test case, Part 2: zero flux oscillatory blowing, AIAA Paper No. 2005-0485